

ModEL: A Modularized End-to-end Reinforcement Learning Framework for Autonomous Driving

Guan Wang^{1†}, Haoyi Niu^{1†}, Desheng Zhu², Jianming Hu³, Xianyuan Zhan^{3✉} and Guyue Zhou^{3✉}

Abstract—Heated debates continue over the best autonomous driving framework. The classic modular pipeline is widely adopted in the industry owing to its great interpretability and stability, whereas the end-to-end paradigm has demonstrated considerable simplicity and learnability along with the rise of deep learning. We introduce a new modularized end-to-end reinforcement learning framework (ModEL) for autonomous driving, which combines the merits of both previous approaches. The autonomous driving stack of ModEL is decomposed into perception, planning, and control module, leveraging scene understanding, end-to-end reinforcement learning, and PID control respectively. Furthermore, we build a fully functional autonomous vehicle to deploy this framework. Through extensive simulation and real-world experiments, our framework has shown great generalizability to various complicated scenarios and outperforms the competing baselines.¹

I. INTRODUCTION

The past decade has witnessed a surge of research interests in end-to-end autonomous driving systems [1]. Despite its appealing simplicity and learnability, most attempts have shown limited performance or adaptability in real-world scenarios due to the large visual [2] and dynamics [3] gaps between simulation and real-world environment. These unsolvable issues remind us of the conventional modular pipeline [4] that decomposes the system into modules for error-tracking and enables autonomous vehicles to behave predictably. However, this approach also leads to a considerable amount of human engineering in devising complicated rules and model fine-tuning. This naturally motivates us to consider a modularized end-to-end architecture [5], [6], i.e. decompose into a scene understanding module, an end-to-end driving planning module trained by imitation learning (IL) or reinforcement learning (RL), and a low-level controller.

Previous works on developing end-to-end autonomous driving systems are primarily using IL for driving planning or control [5]–[11]. Learning an IL policy does not need a high-fidelity simulator, but involves arduous real driving data collection. It is also impossible to outstanding human expert and has limited adaptability in diverse real-world scenarios.

[†]Work done with equal contribution.

¹Guan Wang and Haoyi Niu are with the Department of Computer Science and Technology, and Automation respectively, Tsinghua University, 100084 Beijing, China {wangguan19, niuhy18}@mails.tsinghua.edu.cn

²Desheng Zhu is with the School of Mechanical Electronic and Information Engineering, China University of Mining and Technology, Beijing, China zhuds1996@163.com

³Jianming Hu, [✉]Xianyuan Zhan, and [✉]Guyue Zhou are with Tsinghua University, Beijing, China {hujm, zhanxianyuan, zhouguyue}@mail.tsinghua.edu.cn

¹Please visit <http://carzero.xyz> for the supplementary video.

The huge success of RL has provided another appealing direction. RL has achieved superhuman performance in solving complex tasks [12] [13] in recent years, and also begins to show its potential on safety-critical tasks like autonomous driving [14]. RL can alleviate some major headaches of IL, such as distribution shift problem [15], data bias [16], and causal confusion [17]. Despite the strong capability of RL, developing a real-world end-to-end autonomous driving system using RL remains to be a highly challenging task. Considerable efforts need to be made to properly address the sim2real gap involved during the interactive training of RL policies with a simulator.

In this paper, we present a deployed **Modularized End-to-end Reinforcement Learning Framework (ModEL)** for autonomous driving. The architecture of ModEL is modularized into three parts: 1) **Perception Module** copes with the raw input from a monocular camera and use advanced scene understanding models [18] to perform drivable space and lane boundary identification; 2) **Planning Module** maps the scene understanding outputs to driving decisions via a trained RL policy (Soft Actor-Critic (SAC) [19], the SOTA method of model-free RL); 3) **Control Module** uses mature PID controllers to regulate and control the low-level driving commands given the high-level planning decisions. The modularized framework of ModEL offers a nice solution to address all the aforementioned challenges. First, the decomposition of perception, planning, and control modules reduces the complexity of each individual task while improving the stability and interpretability of the system. Second, the RL algorithm is learned with post-perception outputs together with domain generalization techniques (domain randomization [20] and data augmentation [21]), which greatly reduces the impact of the sim2real issue, while fully exploiting the strength of RL policy learning.

In addition to the introduction of the ModEL framework, this study makes a major contribution by building a real autonomous vehicle that deploys ModEL to support real-world validation. We also design a new distributed training scheme that greatly accelerates the RL training and allows “learning to drive in less than one day”. We examine our method against multiple baselines in CARLA simulator [22] with intentionally introduced visual and dynamics gaps. In the real-world validation experiments, our system proves to be capable of generalizing to diverse complicated scenarios with varying road topology and lighting conditions, as well as the presence of obstacles. Through systematic simulation and real-world evaluation, ModEL demonstrates superior performance that exceeds all the competing baselines.

II. RELATED WORK

A. Modular VS End-to-End Autonomous Driving

Currently, mainstream architectures for autonomous driving are structured in either a modular or an end-to-end way.

The conventional **modular pipeline** comprises a multitude of sub-systems, such as environment perception, localization, behavior prediction, planning, and control [4], [23]. In order to handle as many real-world scenarios as possible, the interoperation of these highly functional modules relies on human-engineered deterministic rules. The first in-depth discussions and analyses of the low-level software that encapsulates these rules are in the 2005 DARPA Grand Challenge [24] and 2007 DARPA Urban Challenge [25], which form a basis for many later studies [4]. The modular pipeline is widely adopted in the industry due to its remarkable interpretability. It endows the overall system with the ability to track down and locate sub-system malfunctions. Nevertheless, modular formalism bears several major drawbacks [1]. Large amounts of human engineering are involved to fine-tune individual and cross-module configurations. The framework also suffers from severe compounding errors when decomposing the whole system into lots of smaller-scale but interpretable modules, as the perception uncertainty and modeling errors could be amplified and passed down through the pipeline.

Alternatively, **end-to-end** autonomous driving has been increasingly acknowledged. It is widely accepted that human driving is a behavior reflex task [1] that requires little high-level reasoning and conscious attention, which harbors the same view with the end-to-end architecture. As a deep learning-based solution, the task-specific end-to-end learning ability brings a great reduction of human engineering efforts. However, many studies [6], [26], [27] recognize the drawback of lack of interpretability in the development of end-to-end systems due to its black-box learning scheme. To alleviate this limitation, Chen *et al.* [28] combine the probabilistic graphical modeling with RL to improve the interpretability for autonomous driving in simulation scenarios. Despite these efforts, weak interpretability remains a fatal disadvantage of the end-to-end approaches against the modular architecture [27].

Based on the above comparisons, there is a growing consensus among researchers that combining the merits of both modular and end-to-end formalism could be a promising solution. The raw perceptual inputs are processed using semantic segmentation methods [18], the intermediate outputs are then used for waypoints planning [6] or control decision learning [29] in an end-to-end manner. This combined framework alleviates the drawbacks of both approaches and offers enhanced learnability, robustness, and even transferability.

B. Imitation Learning VS Reinforcement Learning

In end-to-end framework, **imitation learning** (IL) [5]–[11] has been identified as a practical paradigm for autonomous driving. It uses a supervised learning scheme that imitates the human experts’ demonstrations using algorithms like

behavior cloning (BC) [29]–[31]. IL is known to have several major disadvantages [1]. First, since IL performs supervised learning on training dataset, when facing unseen scenarios during closed-loop testing, serious *distribution shift* problems [15] take place and the agent has no idea what to do. Second, *data bias* [16] deeply hurts the generalizability of IL policy, as the training process pays little attention to rare and risky scenarios, namely the long-tailed problem in self-driving [32]. Finally, *causal confusion* [17] is another problem that occurs in IL, as it performs pure data fitting and handles spurious correlations in data badly. Due to the above limitations, typical IL models can succeed in simple tasks like lane following but underperform in more complicated and rare traffic events. To improve the performance in harder scenarios, conditional imitation learning (CIL) [27], [33], [34] introduces a latent state to fully explain the data, thus resulting in a better model expressiveness. However, due to the lack of the ability to perform long-term predictive “reasoning”, it still has some safety issues during closed-loop testing [34].

Due to the ability to solve complex tasks as well as perform long-term optimization, **reinforcement learning** (RL) has become another popular choice for investigating end-to-end autonomous driving [14], [35]–[37]. RL learns how to map observations to optimized actions by maximizing the expected cumulative reward [38], and can learn strong policies in a simulator without real-world labels [39], [40]. Although RL has lower data efficiency than IL, it could be easily implemented in some high-fidelity simulators, e.g. CARLA [22], where agents can explore in more diverse scenarios. This interactive learning ability resolves the distribution shift, data bias, and causal confusion issues in IL. However, RL is also much harder to train in hard tasks. A modularized framework with a dedicated perception module that performs scene understanding can effectively ease the burden of RL, and also lead to more stable policies. Furthermore, due to the interactive learning nature of RL and its reliance on a simulator, considerable efforts need to be taken to properly address the sim2real gap issue in a deployable autonomous driving system.

III. DETAILED IMPLEMENTATION

The overall architecture of ModEL is described in Fig. 1, consisting of three modules: **(1) Perception Module:** we modify the advanced autonomous vehicle semantic segmentation model DeepLabv3+ [41] with EfficientNet-B0 [42] backbone to perform drivable space and lane boundary estimation based on the input image x from the raw monocular camera. **(2) Planning Module:** using the learned representation z from perception, we use state-of-the-art reinforcement learning algorithm, SAC [19], with specially designed actor, critic network structure to learn the optimized high-level vehicle control actions a , consisting of throttle τ and steering angle θ . Moreover, domain generalization methods are applied to improve generalization. **(3) Control Module:** lastly, the control module maps high-level actions

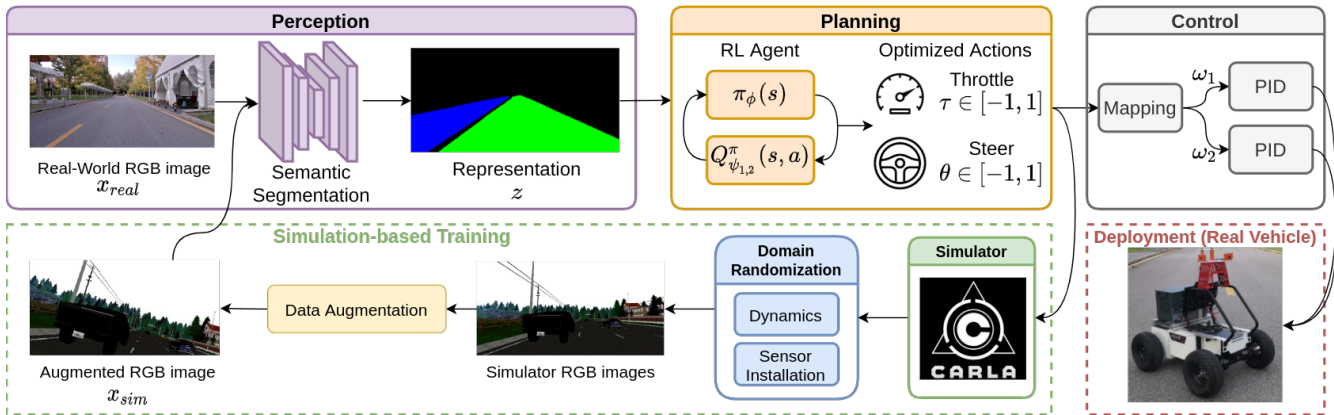


Fig. 1: Overall Architecture of ModelEL

a to low-level vehicle control commands according to the vehicle physical properties using PID controllers.

A. Hardware Setup

Our autonomous vehicle is built upon an Agile.X HUNTER Unmanned Ground Vehicle (UGV) with an on-board computer (i7-9700 CPU, 32GB RAM, GeForce RTX 3060 GPU) and a front monocular RGB camera. The onboard computer runs all system modules based on Robot Operating System (ROS) [43], connected with UGV hardware by Controller Area Network (CAN). Additionally, as all modules are required to run in real-time, we utilize quantization and computational graph optimization techniques [44] to improve model inference latency. The whole system has end-to-end latency (from sensor data collection to low-level control output) of 40ms and runs with a 100ms control interval. The setup of the physical system is detailed in the Appendix.

B. Perception Module

The perception module acts as a powerful supervised state-encoder that maps camera captured RGB images from simulation x_{sim} or real world x_{real} RGB images to a semantically meaningful representation z , effectively bridging visual gap between simulation and real world. Compared to unsupervised state-encoders like image translation networks adopted by previous work [40], using supervised computer vision approaches yields human-readable intermediate representations, which contains cleaner and more precise information needed for the planning module. It is also less impacted by the visual gap, thus more reliable.

We choose the results of drivable area segmentation and lane boundary identification [45] as the intermediate representation z , as it is an effective way to represent road situations from monocular RGB images and is widely used in autonomous driving systems. It labels every pixel as drivable (lane or area currently occupied by ego-vehicle), alternatively drivable (requires a lane-change), or non-drivable (blocked by obstacles). This scheme provides the vehicle with obstacles, lane boundaries, as well as lane change information.

We build our semantic segmentation model based on DeepLabv3+ [41]. It utilizes atrous convolution to enlarge receptive field and capture multi-scale context, along with

encoder-decoder architecture for sharper fine-grained details. It has state-of-the-art performance on autonomous vehicle semantic segmentation datasets. As the ResNet101 backbone in DeepLabv3+ is way too heavy, which is not efficient enough to be deployed in our vehicle, we utilize a new backbone network produced by recent neural architecture search techniques, specifically, the EfficientNet-B0 [42]. Our modification achieves superior accuracy over original DeepLabv3+ and ordinary segmentation models, as shown in the results of Table I. The segmentation model is trained on the open real-world dataset BDD100k [45]. Our model also has great computational efficiency, capable of running at 31 frames per second on the onboard computer.

TABLE I: Perception Model Comparison

Method	mIoU/% (validation)	Inference time (ms)
UNet (ResNet101) [46]	87.2	64
DeepLabv3+ (ResNet101) [41]	92.5	50
Ours (EfficientNet-B0)	93.4	32

C. Planning Module

Our planning module is trained in the simulator CARLA [22] via reinforcement learning but with specially designed domain generalization scheme to abridge the sim2real generalization gap. It chooses best high-level control actions (throttle and steering angle) according to the intermediate representation from the perception module.

1) *Reinforcement learning:* We frame our autonomous vehicle planning task as a Markov Decision Process (MDP) problem and solve it via RL. The problem is represented as a tuple (S, A, r, T, γ) , where S and A denote the state and action set, $r(s, a)$ is the reward function, $T(s'|s, a)$ denotes the transition dynamics, and $\gamma \in (0, 1)$ is the discount factor. In our problem, S , A and r are defined as follows:

States S : as illustrated in Figure 1, we use the drivable area segmentation image z outputted from the perception module, concatenated with the vehicle speed v as the state.

Actions A : We consider the steering angle θ and throttle τ of vehicle as actions $a = [\theta, \tau]$, where $\theta, \tau \in [-1, 1]$.

Reward function r : The design of our reward function involves four parts, including speed control r_{speed} , lane center keeping r_{center} , heading direction alignment $r_{heading}$

as well as collision and undesired lane crossing penalty $r_{penalty}$. For simplicity, we omit the state-action inputs (s, a) in the reward function and described each part as follows: `leftmargin=*,topsep=0pt`

- *Speed control*: Instruct the vehicle with current speed v to drive in the desired speed range, $[v_{min}, v_{target}]$. If it drives too slow, or too fast, the reward will decay linearly. v_{max} indicates maximum possible speed.

$$r_{speed} = \begin{cases} \frac{v}{v_{min}} & \text{if } v < v_{min} \\ 1 & \text{if } v_{min} \leq v \leq v_{target} \\ 1 - \frac{v - v_{target}}{v_{max} - v_{target}} & \text{if } v > v_{target} \end{cases}$$

- *Lane center keeping*: Instruct the vehicle to drive in the center of a lane. d is the current distance from vehicle to lane center and d_{max} is the maximum in-lane distance.

$$r_{center} = \text{Clip}\left(1 - \frac{d}{d_{max}}, 0, 1\right)$$

- *Heading direction*: Instruct the vehicle to drive aligned with a lane. α is the heading angle difference between the vehicle and the lane, with the maximum value α_{max} .

$$r_{heading} = \text{Clip}\left(1 - \frac{\alpha}{\alpha_{max}}, 0, 1\right)$$

- *Collision and undesired lane crossing penalty*: Finally, we define the collision and undesired lane crossing penalty $r_{penalty}$ as follows, where $\mathbf{I}(\cdot)$ is the incident indicator:

$$r_{penalty} = 25 \times \mathbf{I}(\text{collision}) + 12 \times \mathbf{I}(\text{cross solid line}) + 15 \times \mathbf{I}(\text{cross double solid line})$$

The total reward is the multiplication of $r_{speed}, r_{center}, r_{heading}$ and subtracted by collision and undesired lane crossing penalty. The multiplication of the first three objectives is to enforce a soft binary AND logic [47], expecting the agent to do well in all these aspects. The final reward is given as:

$$r = r_{speed} \cdot r_{center} \cdot r_{heading} - r_{penalty}$$

We solve this MDP problem using the Soft Actor-Critic (SAC) algorithm [19], which is a state-of-the-art model-free RL algorithm for continuous action control. As an actor-critic algorithm, SAC learns an actor policy $\pi_\phi(s)$ and an ensemble of critic Q-functions $Q_{\psi_i}^\pi, i = 1, 2$. SAC is derived from the maximum entropy reinforcement learning, which encourages stronger exploration thus leads to better performance. It aims to find an optimal policy that maximizes the following objective:

$$J_\pi(\phi) = \mathbb{E}_s \mathbb{E}_{a \sim \pi_\phi} [Q_{\psi_i}^\pi(s, a) - \lambda \log \pi_\phi(s)]$$

SAC simultaneously trains the critics $Q_{\psi_1}^\pi, Q_{\psi_2}^\pi$ to minimize the soft Bellman residual:

$$J_Q(\psi_i) = \mathbb{E}_{s, a} [Q_{\psi_i}^\pi(s, a) - (r + \gamma Q_{target})]^2$$

$$Q_{target} = \min_{i=1,2} [Q_{\psi_i}^\pi(s', a') - \lambda \log \pi_\phi(s')]$$

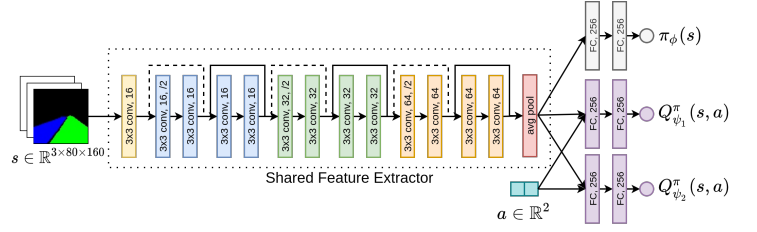


Fig. 2: Neural networks are used in the RL modeling. Residual connections, global average pooling, and shared feature extractor are utilized for $Q_{\psi_i}^\pi$ and π_ϕ to achieve better data efficiency and generalization.

To further improve the function approximation capability and model expressiveness, We design a light-weighted ResNet architecture for both actor and critic networks (see Fig. 2). As our RL task involves understanding complex image-based state information, a more expressive network structure is critical for enhancing the RL agent’s generalization ability [48]. Previous deep network architectures used in image-based RL tasks [12] typically place over 90% parameters on fully-connected layers. We utilize global average pooling to reduce the fully-connected parameters’ size to less than 10%, placing most parameters on more trainable residual layers, thus improving learning efficiency and generalization.

2) *Domain Generalization*: It is known that RL is prone to overfit the training environment and generalizes poorly to unseen scenarios [48]. As the RL policy learned in a simulator needs to be deployed to unseen real-world scenarios, we focus on improving its generalizability by introducing various domain generalization methods during training.

We randomize the configurations in the simulation environment every epoch, to force the agent to adapt to environments with diverse properties, and also avoid overfitting on certain configurations. At sensor level, camera position is randomly chosen from a pre-specified range, to reflect sensor installation errors in real world. Vehicle physical properties (size, mass, etc.) are also randomly chosen from a pre-determined set to reduce the sensitivity to vehicle dynamics. Last but not the least, we apply data augmentations to agent observations, such as rotating the observed image, which contributes a lot to data efficiency and generalization [21].

3) *RL Training Acceleration*: Training an RL agent to solve complex tasks like autonomous driving involves extensive amount of computation. We develop a new distributed framework, which enables highly efficient training of off-policy RL algorithms. Compared to current distributed RL frameworks that synchronize the execution of training procedures, our framework separates environment, actor and optimizer as individual nodes, exchange messages among nodes, while executing asynchronously as fast as possible. Detailed information about the distributed computation framework is discussed in the Appendix.

With our distributed acceleration techniques, we can successfully train the whole system in less than one day on a workstation with 2 GPUs. The training times of different modules are reported in Table II.

TABLE II: Wall-clock Training Time of Modules

ModEL	Perception III-B	Planning (RL) III-C
Time/h	5.1	15.0

D. Low-level Control Module

On our test autonomous vehicle, we first apply a low-pass filter on high-level control actions θ, τ from the planning module to smooth out noisy signals. The outputs are then mapped to vehicle wheel speed ω_1 and steering servo angle ω_2 based on physical properties of the vehicle. Finally, we utilize two PID controllers to follow low-level control targets.

IV. EVALUATION

In this section, we present the baselines, evaluation metrics information and detailed experiment results quantitatively.

A. Experiment Settings

1) *Baselines*: We consider three baselines in this study, including modularized imitation learning (IL) [6], end-to-end IL [7] and RL [22], [49] methods. We re-implement the IL and RL modules of these baselines in our framework for a thorough comparison.

For the training of all IL-based baselines, we follow the treatment described in [6]. We collect 28h of driving data using a privileged modular pipeline as expert (has access to ground-truth map and obstacle information) provided by CARLA [22], and add noise to 20% of the expert control outputs to improve the robustness of the learned policy [33]. For RL-based baselines, all environment and agent configurations are set the same as our proposed approach.

2) *Evaluation Metrics*: For performance evaluation, we use the following metrics: leftmargin=*,topsep=0pt

- **MPI (m)**: meters per intervention, indicating the level of autonomy of the vehicle, which is widely adopted in real-world autonomous vehicle testing. Interventions are performed when collisions happen or the vehicle doesn't move in more than one minute.
- **SR (%)**: success rate, referring to the proportion of travelled distance from the start to the first intervention with respect to the whole journey in one trial.
- **Std[θ] (°)**: the standard deviation of the steering angle, reflecting the lateral smoothness of the trajectory.
- **Std[v] (m/s)**: the standard deviation of the velocity, revealing the longitudinal smoothness of the trajectory.

B. Comparison in Simulation

The main challenge of deploying a simulator-trained system to real world is the visual, vehicle dynamics and scenario gap. Previous simulation-based autonomous driving benchmarks, such as *NoCrash* [16] and CARLA benchmark [22], do not reflect such challenges effectively. For example, the training and test scenarios are visually similar, and not suited well for comprehensive real-world deployment validation.

We propose a new *NoGap* benchmark to measure the sim2real gaps explicitly and provide better real-world generalization evaluations. In *NoGap* benchmark, the autonomous



(a) Training

(b) Testing

Fig. 3: Examples from the *NoGap* benchmark. Training scenarios use game-like low-quality coarse rendering, while testing scenarios are photo-realistic.

driving system is trained in "simulator" and then tested in "real-world" (simulator with different configurations). The evaluation settings are described as follows:

leftmargin=*,topsep=0pt

- **Visual Gap**: We use different simulator rendering modes to create intentionally introduced visual gaps. During training, low-quality coarse rendering is used, producing game-like images. While in testing, the simulator is switched to photo-realistic rendering, producing images that look like real-world. Please refer to Fig. 3 for examples.
- **Dynamics Gap**: Vehicle physical properties are randomly chosen at the beginning of every testing episode, to validate generalization between different vehicle dynamics.
- **Scenario Gap**: 7 CARLA maps are used for training, and 1 reserved for testing, to reflect scenario difference.

We use the MPI metric in simulation evaluations. Inspired by [16], the environment is reset to move the vehicle to a safe state after an intervention for precise intervention counting. Moreover, background vehicles controlled by modular pipeline in CARLA are generated to emulate real-world traffic and dynamic obstacles.

As shown in Table III, end-to-end frameworks fail to generalize from training to testing scenarios due to large visual gaps in RGB inputs. Furthermore, training RL with RGB images is also a much harder task because of too much information contained, which has poorer performance compared with end-to-end IL. Modularized frameworks generalize well under visual gaps and different maps. They also have higher performance in training because of better state representation. Due to stronger model capability and better exploration than IL, modularized RL method achieves the best performance with high degree of generalization.

TABLE III: Evaluation results in simulation, metrics are averaged over 50 runs.

Framework	Input	Planning	MPI	
			Train	Test
End-to-end IL [7]	RGB	IL	134.6	16.2
End-to-end RL [22], [49]	RGB	RL	24.9	0.4
Modularized IL [6]	Perception	IL	306.6	180.9
Modularized RL (Ours)	Perception	RL	449.4	332.6

TABLE IV: Real world evaluation (> means no intervention over the whole trajectory with specified total length.)

Real World Task			Framework							
Road Topology	Obstacle Setup	Lighting Condition	Modularized IL (MIL) [6]				Modularized RL (ModEL)			
			MPI (m)	SR (%)	Std[θ] ($^\circ$)	Std[v] ($m \cdot s^{-1}$)	MPI (m)	SR (%)	Std[θ] ($^\circ$)	Std[v] ($m \cdot s^{-1}$)
Straight	\times	Day	92.1	48.9	1.30	0.30	>1163.5	100.0	1.72	0.19
	\times	Night	187.1	49.0	1.67	0.18	>1304.5	100.0	1.89	0.20
	\checkmark	Day	4.1	16.7	1.25	0.37	34.5	75.0	2.59	0.30
Turn	\times	Day	7.2	53.2	3.03	0.32	>214.9	100.0	3.81	0.23



Fig. 4: The bird’s eye views, actual scenarios, raw inputs, and semantic segmentation results (from left to right) for the tasks in Table IV respectively

C. Real World Benchmark

To evaluate the autonomous driving framework on our test vehicle described in Section III-A, we categorize the real world tasks based on different attributes: road topology (straight and turn), obstacles setup (with obstacle ahead), and lighting condition (day-time and night-time). We test our ModEL framework with the most competitive baseline standing out from simulation evaluation in Section IV-B, the modularized IL (MIL) [6], under the same set of tasks.

To assess the lane-keeping ability on straight and turning roads, we run the vehicle five trials per framework for each non-obstacle task, during each of which we set the vehicle to a collision-free position as close as possible to the place where the intervention takes place. The obstacle setup is implemented as the vehicle accelerates from 0m/s and tries to circumvent the obstacle 5m ahead. If the vehicle successfully bypasses the obstacle, we record it as a successful trial and reset the vehicle to the initial location for the next trial. Otherwise, it commits a failed trial and counts one more intervention. Table IV presents the comparisons about the real world generalizability between the MIL and our ModEL on tasks with different attribute settings.

Several observations can be drawn from these experimental results. ModEL achieves much higher MPI and SR on every task, superior to MIL in terms of autonomy and safety.

ModEL is also generalizable to different lighting conditions, whereas surprisingly, MIL at night-time visibly outperforms itself at day-time. ModEL also has smaller velocity std in most of the tasks, while the more conservative MIL has more hold-backs during the real-world tests. Finally, it is observed that ModEL has better ability to bypass the obstacles. This results in larger std of steering angle of ModEL than the more conservative MIL, as MIL directly bumps into the obstacle and scrapes the curb at turns more often.

We also perform qualitative real-world evaluation on complex and unseen scenarios, such as sidewalk, crowded road and garage. ModEL can handle lane-following, turning and dynamic obstacle avoidance smoothly, revealing good generalization performance. Please refer to supplementary videos and Appendix for details.

V. CONCLUSION

In this paper, we propose a novel deployed modularized end-to-end RL framework, ModEL, for autonomous driving. By combining modular pipeline with state-of-the-art reinforcement learning, we alleviate the challenging sim2real gap, enhance perception performance, and improve RL planning abilities. We also build a test autonomous vehicle to deploy our framework for real-world validation. Additionally, we develop a distributed RL acceleration framework to train

the whole system in less than one day on a single workstation. We validate the performance and generalizability of our framework in simulation with intentionally introduced visual and dynamics gaps. Furthermore, our framework could generalize to diverse and unseen complex real-world scenarios. It also achieves superior performance compared with various end-to-end and imitation learning baselines.

REFERENCES

- [1] A. Tampuu, T. Matiisen, M. Semkin, D. Fishman, and N. Muhammad, "A survey of end-to-end driving: Architectures and training methods," *IEEE Transactions on Neural Networks and Learning Systems*, pp. 1–21, 2020. **1, 2**
- [2] K. Rao, C. Harris, A. Irpan, S. Levine, J. Ibarz, and M. Khansari, "R1-cycleGAN: Reinforcement learning aware simulation-to-real," in *2020 IEEE/CVF Conference on Computer Vision and Pattern Recognition (CVPR)*, 2020, pp. 11 154–11 163. **1**
- [3] X. B. Peng, M. Andrychowicz, W. Zaremba, and P. Abbeel, "Sim-to-Real Transfer of Robotic Control with Dynamics Randomization," *Proceedings - IEEE International Conference on Robotics and Automation*, pp. 3803–3810, 2018. **1**
- [4] J. Levinson, J. Askeland, J. Becker, J. Dolson, D. Held, S. Kammel, J. Z. Kolter, D. Langer, O. Pink, V. Pratt, M. Sokolsky, G. Stanek, D. Stavens, A. Teichman, M. Werling, and S. Thrun, "Towards fully autonomous driving: Systems and algorithms," in *2011 IEEE Intelligent Vehicles Symposium (IV)*, 2011, pp. 163–168. **1, 2**
- [5] J. Huang, S. Xie, J. Sun, Q. Ma, C. Liu, D. Lin, and B. Zhou, "Learning a decision module by imitating driver's control behaviors," in *Proceedings of the Conference on Robot Learning (CoRL) 2020*. **1, 2**
- [6] M. Müller, A. Dosovitskiy, B. Ghanem, and V. Koltun, "Driving Policy Transfer via Modularity and Abstraction," no. CoRL, 2018. [Online]. Available: <http://arxiv.org/abs/1804.09364> **1, 2, 5, 6**
- [7] M. Bojarski, D. Testa, D. Dworakowski, B. Firner, B. Flepp, P. Goyal, L. Jackel, M. Monfort, U. Muller, J. Zhang, X. Zhang, J. Zhao, and K. Zieba, "End to end learning for self-driving cars," *ArXiv*, vol. abs/1604.07316, 2016. **1, 2, 5**
- [8] P. Anderson, A. Chang, D. S. Chaplot, A. Dosovitskiy, S. Gupta, V. Koltun, J. Kosecka, J. Malik, R. Mottaghi, M. Savva, and A. R. Zamir, "On Evaluation of Embodied Navigation Agents," pp. 1–11, 2018. [Online]. Available: <http://arxiv.org/abs/1807.06757> **1, 2**
- [9] S. Hecker, D. Dai, A. Liniger, M. Hahner, and L. Van Gool, "Learning accurate and human-like driving using semantic maps and attention," *IEEE International Conference on Intelligent Robots and Systems*, pp. 2346–2353, 2020. **1, 2**
- [10] Z. Huang, C. Lv, Y. Xing, and J. Wu, "Multi-Modal Sensor Fusion-Based Deep Neural Network for End-to-End Autonomous Driving with Scene Understanding," *IEEE Sensors Journal*, vol. 21, no. 10, pp. 11 781–11 790, 2021. **1, 2**
- [11] Y. Wang, D. Zhang, J. Wang, Z. Chen, Y. Li, Y. Wang, and R. Xiong, "Imitation Learning of Hierarchical Driving Model: From Continuous Intention to Continuous Trajectory," *IEEE Robotics and Automation Letters*, vol. 6, no. 2, pp. 2477–2484, 2021. **1, 2**
- [12] V. Mnih, K. Kavukcuoglu, D. Silver, A. A. Rusu, J. Veness, M. G. Bellemare, A. Graves, M. Riedmiller, A. K. Fidjeland, G. Ostrovski, S. Petersen, C. Beattie, A. Sadik, I. Antonoglou, H. King, D. Kumaran, D. Wierstra, S. Legg, and D. Hassabis, "Human-level control through deep reinforcement learning," *Nature*, vol. 518, no. 7540, pp. 529–533, 2015. [Online]. Available: <https://doi.org/10.1038/nature14236> **1, 4**
- [13] D. Silver, T. Hubert, J. Schrittwieser, I. Antonoglou, M. Lai, A. Guez, M. Lanctot, L. Sifre, D. Kumaran, T. Graepel, *et al.*, "A general reinforcement learning algorithm that masters chess, shogi, and go through self-play," *Science*, vol. 362, no. 6419, pp. 1140–1144, 2018. **1**
- [14] B. R. Kiran, I. Sobh, V. Talpaert, P. Mannion, A. A. Sallab, S. Yogamani, and P. Perez, "Deep Reinforcement Learning for Autonomous Driving: A Survey," *IEEE Transactions on Intelligent Transportation Systems*, no. February, 2021. **1, 2**
- [15] S. Ross, G. Gordon, and D. Bagnell, "A reduction of imitation learning and structured prediction to no-regret online learning," in *Proceedings of the Fourteenth International Conference on Artificial Intelligence and Statistics*, ser. Proceedings of Machine Learning Research, G. Gordon, D. Dunson, and M. Dudík, Eds., vol. 15. Fort Lauderdale, FL, USA: PMLR, 11–13 Apr 2011, pp. 627–635. [Online]. Available: <http://proceedings.mlr.press/v15/ross11a.html> **1, 2**
- [16] F. Codevilla, E. Santana, A. Lopez, and A. Gaidon, "Exploring the limitations of behavior cloning for autonomous driving," *Proceedings of the IEEE International Conference on Computer Vision*, vol. 2019-October, no. Cvc, pp. 9328–9337, 2019. **1, 2, 5**
- [17] P. D. Haan, D. Jayaraman, and S. Levine, "Causal confusion in imitation learning," in *NeurIPS*, 2019. **1, 2**
- [18] M. Cordts, M. Omran, S. Ramos, T. Rehfeld, M. Enzweiler, R. Benenson, U. Franke, S. Roth, and B. Schiele, "The cityscapes dataset for semantic urban scene understanding," in *Proc. of the IEEE Conference on Computer Vision and Pattern Recognition (CVPR)*, 2016. **1, 2**
- [19] T. Haarnoja, A. Zhou, P. Abbeel, and S. Levine, "Soft actor-critic: Off-policy maximum entropy deep reinforcement learning with a stochastic actor," in *Proceedings of the 35th International Conference on Machine Learning*, ser. Proceedings of Machine Learning Research, J. Dy and A. Krause, Eds., vol. 80. PMLR, 10–15 Jul 2018, pp. 1861–1870. [Online]. Available: <http://proceedings.mlr.press/v80/haarnoja18b.html> **1, 2, 4**
- [20] J. Tobin, R. Fong, A. Ray, J. Schneider, W. Zaremba, and P. Abbeel, "Domain randomization for transferring deep neural networks from simulation to the real world," in *2017 IEEE/RSJ international conference on intelligent robots and systems (IROS)*. IEEE, 2017, pp. 23–30. **1**
- [21] M. Laskin, K. Lee, A. Stooke, L. Pinto, P. Abbeel, and A. Srivas, "Reinforcement learning with augmented data," *arXiv preprint arXiv:2004.14990*, 2020. **1, 4**
- [22] A. Dosovitskiy, G. Ros, F. Codevilla, A. Lopez, and V. Koltun, "CARLA: An open urban driving simulator," in *Proceedings of the 1st Annual Conference on Robot Learning*, ser. Proceedings of Machine Learning Research, S. Levine, V. Vanhoucke, and K. Goldberg, Eds., vol. 78. PMLR, 13–15 Nov 2017, pp. 1–16. [Online]. Available: <http://proceedings.mlr.press/v78/dosovitskiy17a.html> **1, 2, 3, 5**
- [23] E. Yurtsever, J. Lambert, A. Carballo, and K. Takeda, "A Survey of Autonomous Driving: Common Practices and Emerging Technologies," *IEEE Access*, vol. 8, pp. 58 443–58 469, 2020. **2**
- [24] S. Thrun, M. Montemerlo, H. Dahlkamp, D. Stavens, A. Aron, J. Diebel, P. Fong, J. Gale, M. Halpenny, G. Hoffmann, and *et al.*, "Stanley: The robot that won the darpa grand challenge," *Journal of Field Robotics*, vol. 23, no. 9, p. 661–692, 2006. [Online]. Available: <https://dx.doi.org/10.1002/rob.20147> **2**
- [25] M. Montemerlo, J. Becker, S. Bhat, H. Dahlkamp, D. Dolgov, S. Ettinger, D. Haehnel, T. Hilden, G. Hoffmann, B. Huhne, and *et al.*, "Junior: The stanford entry in the urban challenge," *Journal of Field Robotics*, vol. 25, no. 9, p. 569–597, 2008. [Online]. Available: <https://dx.doi.org/10.1002/rob.20258> **2**
- [26] É. Zablocki, H. Ben-Younes, P. Pérez, and M. Cord, "Explainability of vision-based autonomous driving systems: Review and challenges," 2021. [Online]. Available: <http://arxiv.org/abs/2101.05307> **2**
- [27] Y. Xiao, F. Codevilla, A. Gurram, O. Urfalioglu, and A. M. Lopez, "Multimodal End-to-End Autonomous Driving," *IEEE Transactions on Intelligent Transportation Systems*, no. 201808390010, pp. 1–11, 2020. **2**
- [28] J. Chen, S. E. Li, and M. Tomizuka, "Interpretable end-to-end urban autonomous driving with latent deep reinforcement learning," *IEEE Transactions on Intelligent Transportation Systems*, pp. 1–11, 2021. **2**
- [29] A. Behl, K. Chitta, A. Prakash, E. Ohn-Bar, and A. Geiger, "Label efficient visual abstractions for autonomous driving," in *IEEE International Conference on Intelligent Robots and Systems*, 2020, pp. 2338–2345. **2**
- [30] A. Prakash, A. Behl, E. Ohn-Bar, K. Chitta, and A. Geiger, "Exploring data aggregation in policy learning for vision-based urban autonomous driving," *2020 IEEE/CVF Conference on Computer Vision and Pattern Recognition (CVPR)*, pp. 11 760–11 770, 2020. **2**
- [31] D. Chen, B. Zhou, V. Koltun, and P. Krähenbühl, "Learning by cheating," in *Proceedings of the Conference on Robot Learning*, ser. Proceedings of Machine Learning Research, L. P. Kaelbling, D. Kragic, and K. Sugiura, Eds., vol. 100. PMLR, 30 Oct–01 Nov 2020, pp. 66–75. [Online]. Available: <https://proceedings.mlr.press/v100/chen20a.html> **2**
- [32] J. Mao, M. Niu, C. Jiang, H. Liang, X. Liang, Y. Li, C. Ye, W. Zhang, Z. Li, J. Yu, *et al.*, "One million scenes for autonomous driving: Once dataset," *arXiv preprint arXiv:2106.11037*, 2021. **2**

- [33] F. Codevilla, M. Müller, A. López, V. Koltun, and A. Dosovitskiy, "End-to-end driving via conditional imitation learning," in *2018 IEEE International Conference on Robotics and Automation (ICRA)*, 2018, pp. 4693–4700. 2, 5
- [34] J. Hawke, R. Shen, C. Gurau, S. Sharma, D. Reda, N. Nikolov, P. Mazur, S. Micklethwaite, N. Griffiths, A. Shah, and A. Kendall, "Urban Driving with Conditional Imitation Learning," *Proceedings - IEEE International Conference on Robotics and Automation*, pp. 251–257, 2020. 2
- [35] Z. Q. Huang, Z. W. Qu, J. Zhang, Y. X. Zhang, and R. Tian, "End-to-End Autonomous Driving Decision Based on Deep Reinforcement Learning," *Tien Tzu Hsueh Pao/Acta Electronica Sinica*, vol. 48, no. 9, pp. 1711–1719, 2020. 2
- [36] B. Osiński, A. Jakubowski, P. Ziecina, P. Miłoś, C. Galias, S. Homoceanu, and H. Michalewski, "Simulation-based reinforcement learning for real-world autonomous driving," in *2020 IEEE International Conference on Robotics and Automation (ICRA)*. IEEE, 2020, pp. 6411–6418. 2
- [37] X. Liang, T. Wang, L. Yang, and E. Xing, "Cirl: Controllable imitative reinforcement learning for vision-based self-driving," in *The European Conference on Computer Vision (ECCV)*, September 2018. 2
- [38] R. S. Sutton, A. G. Barto, *et al.*, *Introduction to reinforcement learning*. MIT press Cambridge, 1998, vol. 135. 2
- [39] X. Pan, Y. You, Z. Wang, and C. Lu, "Virtual to real reinforcement learning for autonomous driving," *British Machine Vision Conference 2017, BMVC 2017*, 2017. 2
- [40] A. Bewley, J. Rigley, Y. Liu, J. Hawke, R. Shen, V. D. Lam, and A. Kendall, "Learning to drive from simulation without real world labels," *Proceedings - IEEE International Conference on Robotics and Automation*, vol. 2019-May, pp. 4818–4824, 2019. 2, 3
- [41] L.-C. Chen, G. Papandreou, I. Kokkinos, K. Murphy, and A. L. Yuille, "Deeplab: Semantic image segmentation with deep convolutional nets, atrous convolution, and fully connected crfs," *IEEE Transactions on Pattern Analysis and Machine Intelligence*, vol. 40, no. 4, pp. 834–848, 2018. 2, 3
- [42] M. Tan and Q. Le, "Efficientnet: Rethinking model scaling for convolutional neural networks," in *International Conference on Machine Learning*. PMLR, 2019, pp. 6105–6114. 2, 3
- [43] Stanford Artificial Intelligence Laboratory et al., "Robotic operating system." [Online]. Available: <https://www.ros.org> 3
- [44] O. R. developers, "Onnx runtime," <https://onnxruntime.ai/>, 2021. 3
- [45] F. Yu, H. Chen, X. Wang, W. Xian, Y. Chen, F. Liu, V. Madhavan, and T. Darrell, "Bdd100k: A diverse driving dataset for heterogeneous multitask learning," in *IEEE/CVF Conference on Computer Vision and Pattern Recognition (CVPR)*, June 2020. 3
- [46] O. Ronneberger, P. Fischer, and T. Brox, "U-net: Convolutional networks for biomedical image segmentation," in *International Conference on Medical image computing and computer-assisted intervention*. Springer, 2015, pp. 234–241. 3
- [47] M. L. Vergara, "Accelerating training of deep reinforcement learning-based autonomous driving agents through comparative study of agent and environment designs," Master's thesis, NTNU, 2019. 4
- [48] K. Cobbe, O. Klimov, C. Hesse, T. Kim, and J. Schulman, "Quantifying generalization in reinforcement learning," in *International Conference on Machine Learning*. PMLR, 2019, pp. 1282–1289. 4
- [49] A. Kendall, J. Hawke, D. Janz, P. Mazur, D. Reda, J.-M. Allen, V.-D. Lam, A. Bewley, and A. Shah, "Learning to drive in a day," in *2019 International Conference on Robotics and Automation (ICRA)*, 2019, pp. 8248–8254. 5

APPENDIX

A. Qualitative real-world experiment scenarios

ModEL proves to be capable of avoiding both regular and unseen obstacles (setup as Fig. 5a) and also achieves superior generalizability on unseen scenarios, such as being exposed to head-on high beams, traveling on sidewalks, through dense crowds, and even in a garage (depicted in Fig. 5b). Please explore our accompanying video for more.

B. Distributed Training Framework

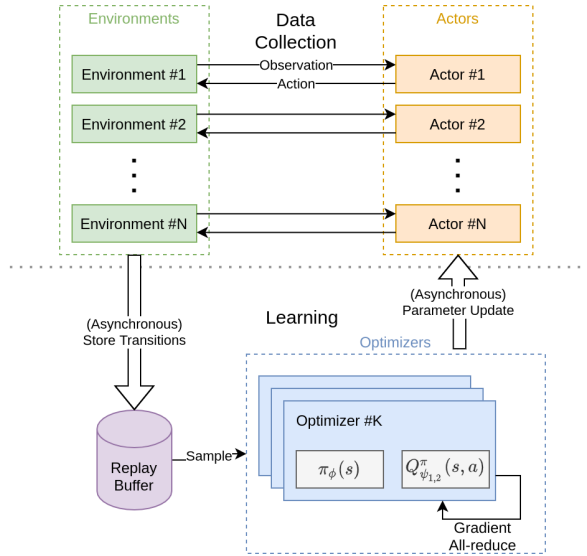


Fig. 6: Distributed training architecture

We developed a distributed off-policy RL training framework (detailed in Fig. 6), enabling highly-efficient RL training. As off-policy RL algorithms can learn from data

generated by older policies, per-step data collection and learning procedure doesn't depend on each other. So we run the two procedures separately as fast as possible. Message exchanging between procedures (transitions storing and policy parameters updating) is asynchronous and delayed. For data collection, N simulation environments and actor instances are created as independent nodes. An environment sends observations to its corresponding actor and receives predicted actions for stepping. For actor and critic learning, K optimizer nodes are instantiated. Each optimizer has the same copy of actor $\pi_\phi(s)$ and critic $Q_{\psi_{1,2}}^\pi(s,a)$ networks, and compute gradients using batches of transitions sampled from the replay buffer, then utilize distributed all-reduce to synchronize gradients for optimization.

C. Hardware implementation details

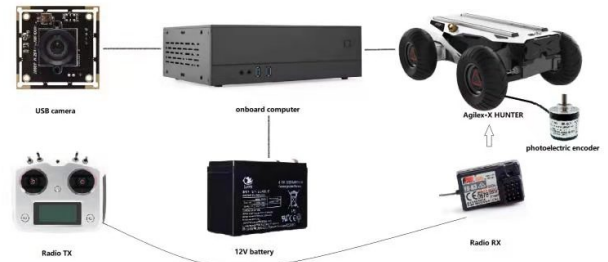


Fig. 7: The overall physical system

The hardware system that deploys ModEL includes a USB front monocular RGB camera (640×480 resolution), an onboard computer (i7-9700 CPU, 32GB RAM, GeForce RTX 3060 GPU), a remote-control unit and an Agile.X HUNTER Unmanned Ground Vehicle (UGV) with photoelectric encoders for wheel odometry, as shown in Figure 7. The whole



(a) Obstacle avoidance tests: barrier, bicycle, motorcycle, dummy, person, and chair-like robot (from left to right)



(b) Test in unseen and complex scenarios: high beam, sidewalk, crowds, and garage scenarios (from left to right)

Fig. 5: Qualitative real-world experiments

system runs on the onboard computer as separated nodes with different functions, using Robot Operating System (ROS) to communicate with each other. The vehicle control node receives vehicle state and sends low-level control commands through Controller Area Network (CAN). The autonomous driving node runs the whole ModEL framework, including sensor data collection, perception, planning and control. The monitor node records vehicle safety state and trajectory statistics.

D. Hyperparameter Setup

Table V lists all hyperparameters used to train the ModEL framework, including both perception and planning module.

TABLE V: Hyperparameters

Parameter	Value
Perception	
model	DeepLabv3+
backbone	EfficientNet-B0
optimizer	Adam
learning rate	10^{-3}
batch size	80
loss	Dice loss
training epochs	45
Planning	
algorithm	Soft Actor-Critic
learning rate	$3 * 10^{-4}$
batch size	256
discount (γ)	0.99
target entropy	-2
replay buffer size	10^6
target smoothing factor (τ)	0.02
update to data ratio	0.5